First published in:

Symbols used

d	[μm]	thickness of cathode
D_i^{eff}	[cm^2s^{-1}]	effective diffusion coefficient of species i
$D_{H_2O,k}$	[cm^2s^{-1}]	Knudsen diffusion coefficient of H_2O
$D_{H_2-H_2O}$	[cm^2s^{-1}]	binary diffusion coefficient of H_2 and H_2O
E	[V]	equilibrium potential
E_0	[V]	standard (reversible) potential
F	[$C\,mol^{-1}$]	Faraday constant ($9.6485 \cdot 10^4$ $C\,mol^{-1}$)
J	[$A\,m^{-2}$]	current density
$J_{0,i}$	[$A\,m^{-2}$]	exchange current density
L	[μm]	thickness of electrolyte
M_i	[$g\,mol^{-1}$]	molar weight of species i ($i = H_2O$ and H_2)
n	[–]	cathode porosity
N_i	[–]	rate of mass transport for species i
P	[atm]	operating pressure
P_i	[atm]	partial pressure of species i ($i = H_2O$, H_2)
r	[μm]	mean pore radius of cathode
R	[$J\,mol^{-1}K^{-1}$]	universal gas constant (8.3145 $J\,mol^{-1}K^{-1}$)
T	[K]	operating temperature
V	[V]	cell potential
x	[–]	depth measured from the cathode surface
y_i	[–]	molar fraction of species i ($i = H_2O$, H_2)
y_i^I	[–]	molar fraction of species i in the bulk ($i = H_2O$, H_2)
$\eta_{act,a}$	[V]	activation overpotential at the anode
$\eta_{act,c}$	[V]	activation overpotential at the cathode
η_{conc}	[V]	concentration overpotential
η_{ohmic}	[V]	ohmic overpotential
ξ	[–]	cathode tortuosity
φ	[Ωm]	electrical resistance of electrolyte
$\sigma_{i,j}$	[Å]	mean characteristic length of species i and j
Ω_D	[–]	dimensionless diffusion collision integral
τ	[–]	dimensionless temperature
$\frac{\varepsilon_i}{k}$	[K]	Lennard-Jones potential of species i ($i = H_2O$ and H_2)

Subscripts

a	anode
c	cathode

References

[1] P. Pfeifer et al., *Chem. Eng. Tech.* **2005**, *28 (4)*, 474. DOI: 10.1002/ceat.200407137
[2] T. Maki, T. Ueyama, K. Mae, *Chem. Eng. Tech.* **2005**, *28 (4)*, 494. DOI: 10.1002/ceat.200407115
[3] K. Shah, X. Ouyang, R. S. Besser, *Chem. Eng. Tech.* **2005**, *28 (3)*, 303. DOI: 10.1002/ceat.200407140
[4] M. Ni, M. K. H. Leung, D. Y. C. Leung, K. Sumathy, *Renew. Sustain. Energy Rev.,* in press. DOI: 10.1016/j.rser.2005.01.009
[5] M. Ni, M. K. H. Leung, K. Sumathy, D. Y. C. Leung, *Int. J. Hydrogen Energy* **2006**, in press. DOI:10.1016/j.ijhydene.2005.11.005
[6] M. A. Khaleel, J. R. Selman, in *HighTemperature Solid Oxide Fuel Cells-Fundamentals, Design and Applications* (Eds: S. C. Singhal, K. Kendall), Elsevier Advanced Technology, The Boulevard, UK **2003**.
[7] M. V. Perfiliev, *Int. J. Hydrogen Energy.* **1994**, *19 (3)*, 227. DOI: 10.1016/0360–3199 (94) 90090–6
[8] S. H. Chan, Z. T. Xia, *J. Appl. Electrochem.* **2002**, *32 (3)*, 339. DOI: 10.1023/A: 1015593326549
[9] E. Hernandez-Pacheco et al., *J. Power Sources* **2004**, *138 (1–2)*, 174. DOI: 10.1016/j.jpowsour.2004.06.051
[10] R. Krishna, J. A. Wesselingh, *Chem. Eng. Sci.* **1997**, *52 (6)*, 861. DOI: 10.1016/S0009–2509 (96) 00458–7
[11] J. W. Veldsink, G. F. Versteeg, W. P. M. Van Swaaij, R. M. J. Van Damme, *Chem. Eng. J. Biochem. Eng. J.* **1995**, *57 (2)*, 115. DOI: 10.1016/0923–0467 (94) 02929–6
[12] H. Yakabe et al., *J. Power Sources* **2000**, *86 (1–2)*, 423. DOI: 10.1016/S0378–7753 (99) 00444–9
[13] R. C. Reid, J. M. Prausnitz, B. E. Poling, *The Properties of Gases & Liquids*, 4th ed., McGraw-Hill Book Company, New York **1987**.
[14] J. R. Ferguson, J. M. Fiard, R. Herbin, *J. Power Sources* **1996**, *58 (2)*, 109. DOI: 10.1016/0378–7753 (95) 02269–4
[15] A. Momma, T. Kato, Y. Kaga, S. Nagata, *J. Ceram. Soc. Jpn.* **1997**, *105 (5)*, 369.
[16] G. Tao et al., *2005 DOE Hydrogen Program Annual Rev.*, Arlington, Virginia, U.S.A., May **2005**.
[17] A. Q. Pham, in *Proc. of the 2000 DOE Hydrogen Prog. Rev.*, U.S.A. **2000**.
[18] A. Vance, *US DOE 2003 Annual Merit Rev. Meeting*, Berkeley, California, U.S.A., May **2003**.
[19] H. Arashi, N. Naito, H. Miura, *Int. J. Hydrogen Energy* **1991**, *16 (9)*, 603. DOI: 10.1016/0360–3199 (91)90083-U
[20] R. Hino, K. Haga, H. Aita, K. Sekita, *Nucl. Eng. Des.* **2004**, *233 (1–3)*, 363. DOI: 10.1016/j.nucengdes.2004.08.029

Comparison of Comminution by Impact of Particle Collectives and Other Grinding Processes

By *Andreas Weber**, *Ulrich Teipel*, and *Hermann Nirschl*

DOI: 10.1002/ceat.200500338

This article presents the innovative grinding apparatus Pulsar in which comminution is caused by impact of a particle plug on an impact plate. Advantages of the Pulsar principle in comparison to other types of mills are discussed. The aim

[*] Dipl.-Ing. A. Weber (andreas.weber@mvm.uka.de), Prof. Dr.-Ing. habil. H. Hirschl, Institut für Mechanische Verfahrenstechnik und Mechanik, Universität Karlsruhe (TH), D-76128 Karlsruhe, Germany; Prof. Dr.-Ing. U. Teipel, Fachbereich Partikeltechnologie, Georg-Simon-Ohm-Fachhochschule Nürnberg, Wassertorstraße 10, D-90489 Nürnberg, Germany.

of the work is to classify the Pulsar system in the field of grinding apparatus and machines in terms of energy consumption. Experiments were carried out in a Pulsar, a cross beater mill and a ball mill for comparison purposes. The results show that, for the material quartz sand, grinding in the Pulsar at a medium pressure of compressed air ($p_{car,i}$ = 7.5 bars) and a medium magnetic valve opening time (t_o = 70 ms) is as efficient as in the ball mill. The grinding energy consumption of both mills, the Pulsar and the ball mill, is remarkably higher than that of the cross beater mill.

1 Introduction

Mechanical comminution processes can be classified by the number of comminution tools [1] resulting in different types of stress:
– two or more tools: pressure and shear stress;
– one tool: impact stress;
– no tool: stress due to the surrounding media.

In mills, where the grinding material is exposed to pressure and shear stresses between two or more tools, the relative velocities causing the stress are comparatively low (< 10 m/s). In other grinding apparatus and machines, particles are comminuted by impact stress events on single tools with stress velocities exceeding 20 m/s.

Another classification criterion is the number of particles stressed in the same event:
– single particles;
– groups of particles.

In breakers, for example, single particles are exposed to pressure and shear stresses with low stress velocities. Pressure and shear stresses cause comminution also in roller mills and in the bed roller mill, but in these cases groups of particles are stressed in the same event. Grinding body mills bear a complex combination of pressure, shear and strike stresses to single particles or particle groups. Comminution by impact stresses of single particles is realized in impact and jet mills where interparticulate collisions are regarded as stressing on one tool.

The Pulsar represents a new type of grinding apparatus where a group of particles is exposed to an impact stress with high stress velocities. The grinding material is comminuted by a combination of impact stresses and interparticulate stresses. In order to compare the Pulsar principle with established grinding machines in terms of grinding energy consumption, experiments were performed in a Pulsar, a cross beater mill and a ball mill.

2 Material and Methods

2.1 Pulsar

The grinding apparatus Pulsar has been presented by Pulsar GmbH Micronizing Systems, Germany [2]. A bulk material is accelerated by a pulse of compressed air in a vertical barrel forming a particle plug. Comminution is caused by the stresses occurring during the deceleration of the particle plug at an impact plate. A schematic display of the experimental setup is shown in Fig. 1.

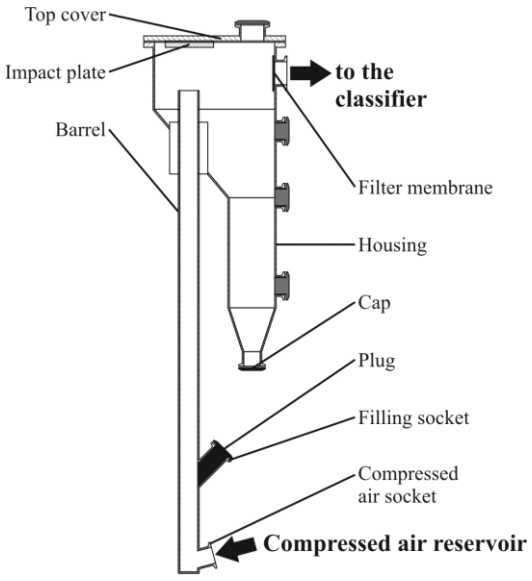

Figure 1. Schematic display of grinding apparatus Pulsar (modified for single shots).

For the present work the Pulsar was modified to enable investigation of single shots. With this method well-defined experimental conditions could be realized. After filling the barrel with the initial material up to the lower end of the filling socket the socket is closed with a plastic plug. Next, the compressed air reservoir is filled to the pressure $p_{car,i}$[1)]. After these preparations, the pneumatic pulse is inducted by shortly opening the magnetic valve (opening time t_o) between the compressed air reservoir and the compressed air socket of the barrel. The pulse of compressed air accelerates the bulk material in the barrel forming a particle plug. After leaving the barrel, the particle plug is decelerated on an impact plate attached to the top cover of the apparatus. The distance between the upper end of the barrel and the impact plate is in the same size range as the length of the particle plug. The outlet of the Pulsar is closed with a filter membrane preventing a high pressure in the apparatus after the single shot. The filter membrane also ensures that the product is kept in the apparatus from which it can be removed for analysis after the experiment.

Particle size distributions were determined by combining two analysis techniques. Particles of > 250 µm were dry-sieved. The fine particles of < 400 µm were analyzed by laser light scattering spectroscopy. For the chosen material the equivalent diameters x were found to be in good agreement for the two analysis techniques.

1) List of symbols at the end of the paper.

As both position and steepness of the cumulative particle size distribution Q_3 change within the experiments, the Sauter mean diameter x_S was chosen as a single measure for the fineness of particle size distributions. A spherical particle with a diameter x_S has the same volume to surface ratio as the total distribution. The Sauter mean diameter x_S was determined from the cumulative mass distributions Q_3:

$$x_S = \left[\sum_j \frac{1}{x_{m,j}} \Delta Q_3(x_{m,j}) \right]^{-1} \quad (1)$$

The smaller the Sauter mean diameter x_S after the experiment, the more new surface was generated due to the breakup of particles.

The comminution result is strongly dependent on the mass-related energy E_M available for the comminution process. For the Pulsar experiments the mass-related energy, E_M, is calculated by measuring the pressure in the compressed air reservoir after the shot $p_{car,f}$. Assuming an adiabatic expansion of the compressed air during the shot and an isothermal filling of the compressed air reservoir between the experiments, the consumption of compressed air per shot is given by the following equation:

$$\Delta V_N = \frac{p_{car,i}}{p_0} \cdot V_{car} \cdot \left\{ 1 - \left(\frac{p_{car,f}}{p_{car,i}} \right)^{1/\kappa} \right\} \quad (2)$$

Under the assumption of adiabatic compression of the compressed air, the mass-related energy E_M can be calculated as follows:

$$E_M = \frac{1}{M} \cdot p_0 \cdot \Delta V_N \cdot \frac{1}{\kappa - 1} \cdot \left\{ \left(\frac{p_{car,i}}{p_0} \right)^{(\kappa-1)/\kappa} - 1 \right\} \quad (3)$$

In the Pulsar the particles in the upper layers of the plug are exposed to impact stresses. Inside the plug particles are comminuted by interparticulate stresses with high velocity gradients. According to theoretical considerations [3] the main comminution should occur in the middle upper part of the plug forming a cone of fine particles that is kept at the impact plate as long as particles from the lower part of the plug keep flowing towards the impact plate. Particles from the border area of the plug are redirected radially away from the middle of the impact plate. Comminution is intensified by pressure due to the deceleration of the lower parts of the particle plug. Therefore, it is important that the plug is as compact as possible when it reaches the impact plate. This means that little axial enlargement due to permeation of air during acceleration and little radial enlargement after the plug has left the barrel enhance comminution.

Previous investigations of grinding in the Pulsar [4] have shown that comminution is enhanced by increasing the pressure in the compressed air reservoir before the shot $p_{car,i}$ and by increasing the magnetic valve opening time t_o. Increasing pressure $p_{car,i}$ leads to higher accelerations resulting in higher velocities of the particle plug at the upper end of the barrel. Therefore, the particle plug exhibits a higher kinetic energy available for comminution. Longer magnetic valve opening times enhance comminution in the Pulsar as the larger volume of compressed air expanding behind the particle plug causes a more uniform acceleration of the different layers of plug and less axial enlargement. Thus, a more compact plug reaches the target plate, leading to intensified comminution due to an enhanced exchange of impulse between the particles that have already reached the impact plate and those in the lower layers of the plug.

As mentioned above, some modifications were made to the laboratory apparatus to enable investigation of single shots with well-defined experimental conditions. Contrary to the laboratory equipment, the bottom of the apparatus housing is connected to the filling socket in the continuously operated Pulsar. In continuous mode the housing is filled with a product bed until half of its height. The product bed ensures the filling of the barrel after each shot and enables multiple stressing of the grinding product. After the impact of a particle plug the coarse particles fall onto the product bed while the fine particles are directed towards the classifier by the air flow. Particles rejected by the classifier are transferred onto the product bed in the apparatus and exposed to stress again like the coarse particles that did not leave the housing.

Grinding in the Pulsar may be advantageous for materials with special demands. The Pulsar can be adapted to increased requirements in terms of avoidance of abrasion. The stress region of the grinding apparatus contains no moving or rotating parts. Coating of inner parts of the apparatus with an abrasion-resistant material can be realized with little effort and investment. After several shots, a cone of fine product is formed in the center of the impact plate. Therefore, the following particle plugs do not impact on the impact plate material but are comminuted quasi-autogenously on this cone of fine product. The critical point of avoidance of abrasion in the Pulsar is the barrel. It has to be adapted to the special requirements of purity by choosing an appropriate barrel material.

The Pulsar has advantages in grinding temperature-sensitive materials as the stressed product is quickly removed from the grinding region. Additionally, the expansion of the compressed air results in a temperature reduction in the barrel, counteracting the heat of friction.

2.2 Cross Beater Mill

From the range of impact mills in which single particles are exposed to series of impact stresses a cross beater mill Retsch SK100 was chosen. It consists of a cross beater with three impact plates rotating in a horizontally assembled cylindrical grinding chamber with profiled walls. The material falls into the grinding chamber through a central hopper. In the chamber the product is comminuted by a series of impacts between the product and the rotor or the profiled walls or by particle-particle collisions. The crushed particles leave the stress region through a sieve insert on the bottom

side of the grinding chamber. Product size and grinding time can be varied by the mesh width of the sieve insert.

To determine the mass-related energy consumption for the comminution in the impact mill, the real power consumption of the mill was monitored as a function of the milling time. Without grinding material the no-load real power P_0 is required to turn the rotor. As soon as grinding material is added, power consumption rises as the rotor turns at the same speed against an additional resistance produced by the grinding material. While the product is leaving the grinding chamber through the sieve insert, resistance and power consumption P decrease exponentially. When the entire product has left the grinding chamber, the no-load real power consumption P_0 is reached again. The mass-related energy consumption for comminution in the cross beater mill can be calculated by an integration of the $P(t)$ plot:

$$E_M = \frac{1}{M} \int P \mathrm{d}t \tag{4}$$

The mesh width of the sieve on the bottom side was varied (4, 6, and 10 mm) within the experimental series. Additionally, investigations were carried out without sieve insert, resulting in even shorter grinding times than with sieve insert.

2.3 Ball Mill

In a ball mill the material is ground by a complex combination of pressure, shear and strike stress series. The experiments were conducted at the Georg-Simon-Ohm Fachhochschule Nürnberg, Germany. The Bond ball mill [5, 6] has a diameter and a length of 305 mm. Monodisperse steel balls were used as grinding media. Two series of experiments were carried out with grinding ball diameters D_{gb} of 17 mm and 22 mm, respectively. The grinding ball filling degree of the mill was 30 % per volume. 100 % of the pores between the grinding balls were filled by the bulk material. The rotational speed of the ball mill was 70 rpm, equalling approx. 90 % of the critical rotational speed.

The Bond ball mill was equipped with a torque measuring device [7]. The mass m_l on a force measuring device was monitored as a function of time. As the signal of m_l swings periodically over the turns due to the mechanical setup of the force measuring device, the median value was used for m_l. The mass-related energy, E_M, for grinding in the ball mill can be calculated by the following equation:

$$E_M = \frac{1}{M} \cdot m_l \cdot g \cdot l \cdot 2\pi \cdot n \tag{5}$$

Besides the grinding ball diameter D_{gb} the number of rotations n and the grinding time were varied within the experimental series.

In a ball mill the grinding balls are dragged along by the rotating grinding chamber. At the chosen rotational speed of 90 % of the critical rotational speed the grinding balls perform a cataract movement. This means that the grinding balls leave the cylindrical wall of the grinding chamber at the point were the gravitational forces exceed the centrifugal forces. The grinding balls fall back onto the moved bed consisting of product and other grinding balls. Heavier and larger grinding balls should enhance comminution as they bear a higher kinetic energy available for comminution when they reach the moved bed.

2.4 Material

Quartz sand, commonly used for grinding investigations, was chosen as material for the comminution experiments. In order to obtain a particle size distribution approximate to that of the equilibrium product in a continuously working Pulsar, the initial material for the investigations was composed of different fractions of quartz sand. The initial material (see Fig. 4) consists of irregular edgy particles with a density of ρ = 2650 kg/m^3, the solids volume fraction of the bulk is δ_0 = 0.61 approximately. The discrete particle size distribution of the initial material shows a distinct maximum at x = 4 mm, the smallest detectable particles have a size of 250 μm. The Sauter mean diameter (see chapter 2.1) of the initial material $x_{S,i}$ is 1006 μm.

3 Results

3.1 Pulsar

Preliminary investigations showed that after three single shots the dead storage of the Pulsar was filled, a cone of fine product had formed in the center of the impact plate and the adhesions of fine particles on the housing wall were in equilibrium. Experiments were used for evaluation only after equilibrium was reached.

For the Pulsar increasing the pressure in the compressed air reservoir before the shot $p_{car,i}$ and increasing the magnetic valve opening time t_o grinding results in enhanced comminution (see chapter 2.1). For comparison of energy consumption three combinations of operating conditions were chosen (see Fig. 2). A relatively low mass-related energy, E_M ($p_{car,i}$ = 5.0 bars, t_o = 50 ms), and a relatively high mass-related energy, E_M ($p_{car,i}$ = 10.0 bars, t_o = 90 ms), were selected to investigate the limits of the Pulsar apparatus. Additionally, experiments with a medium mass-related energy ($p_{car,i}$ = 7.5 bars, t_o = 70 ms) which approximates the conditions of the continuously operated Pulsar were carried out. Fig. 2 shows the cumulative mass distributions Q_3, the mass-related energies E_M and the Sauter mean diameters x_S for the single shot comminution experiments in the Pulsar.

As expected, increasing mass-related energy inputs; E_M; lead to enhanced comminution resulting in larger newly created surfaces indicated by smaller Sauter mean diameters. For $p_{car,i}$ = 5.0 bars and t_o = 50 ms the mass-related energy E_M is very low. Therefore, little comminution occurs, the

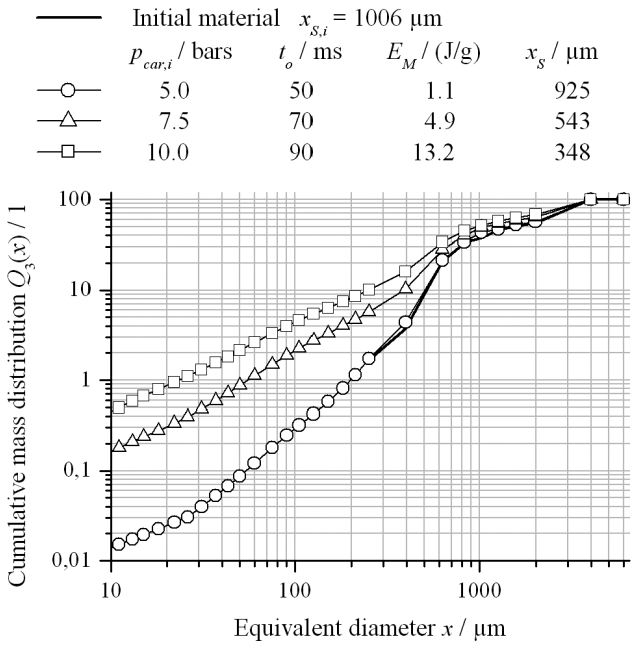

Figure 2. Grinding results for Pulsar: cumulative mass distribution $Q_3(x)$, variation of pressure $p_{car,i}$ and magnetic valve opening time t_o.

Sauter mean diameters of the product and the initial material are nearly the same. It is almost impossible to distinguish the mass distribution of the product and the initial material in the range $x > 250$ µm. The smallest particles of the initial material were 250 µm (see chapter 2.4). For the two other combinations of operating conditions the mass-related energy inputs E_M are high enough to cause remarkable comminution resulting in low Sauter mean diameters compared to the initial material. The highest chosen mass-related energy input E_M resulted in a less steep distribution Q_3 for the fine particles $x < 250$ µm compared to the medium mass-related energy input E_M, indicating a higher relative amount of very fine particles.

3.2 Cross Beater Mill

The mesh width of the sieve insert at the bottom of the grinding chamber has a major influence on grinding time, number of stress events and particle size of the product. In Tab. 1 the Sauter mean diameters and the corresponding mass-related energies E_M of the comminution experiments in the cross beater mill are presented.

Table 1. Grinding results for cross beater mill: Sauter mean diameter x_S, variation of sieve insert mesh width x_{sw}.

Sieve insert mesh width x_{sw}/mm	no insert	10	6	4	Initial material
Sauter mean diameter x_S/µm	215	144	129	96	1006
Mass-related energy E_M/(J/g)	2.4	4.3	5.6	9.1	0

In the experimental series a reduction of the sieve insert mesh width x_{sw} increases the mass-related energy input E_M and enhances comminution illustrated in lower Sauter mean diameters x_S. Even without sieve insert a relatively large new surface is created by breakup of particles. In the corresponding experiment the Sauter mean diameter x_S decreases to approx. a fifth of that of the initial material.

3.3 Ball Mill

The cumulative mass distributions $Q_3(x)$ and the Sauter mean diameters x_S of the products obtained in the Bond ball mill experiments are illustrated in Fig. 3. Increasing the number of rotations n and the grinding time leads to substantially higher amounts of fine products clarified by lower Sauter mean diameters x_S. This meets the expectations as a longer grinding time leads to a higher number of stress events, increased comminution and larger particulate surface because the particles are too big to agglomerate significantly. For the fine particles $x < 100$ µm the steepness of the distributions is approximately the same for the two displayed numbers of rotations n, indicating that no overproportional accumulation of very fine product occurs within the experiments. This is in contrast to the single shot experiments in the Pulsar (see chapter 3.1).

For reasons of clearness, Fig. 3 displays only two different numbers of rotations (n = 140 and n = 560) Additional experimental series were carried out with n = 70 and n = 280 rotations. The results are shown in Fig. 4 and confirm the tendencies of the investigations shown in Fig. 3.

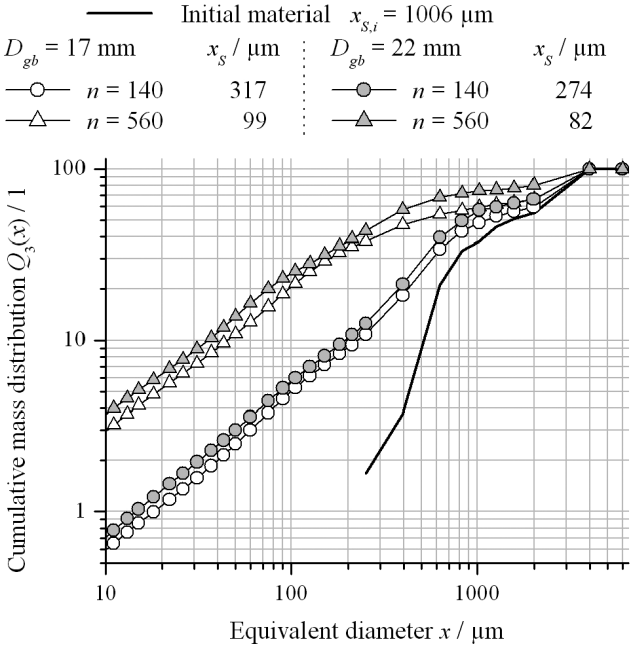

Figure 3. Grinding results for Bond ball mill: cumulative mass distribution $Q_3(x)$, variation of grinding ball diameter D_{gb} and number of rotations n.

3.4 Comparison of Grinding Energy

The ratio of the Sauter mean diameters after to before comminution was chosen as a measure of the comminution progress. The smaller the ratio $x_S/x_{S,i}$ the more new surface was created within the experiment. In Fig. 4 the mass-related comminution energy E_M is plotted as a function of the comminution progress $x_S/x_{S,i}$ for the three grinding apparatus investigated. In that type of display energy-efficient comminution processes can be found at low abscissa and low ordinate values, indicating intense comminution and low energy input.

Grinding in the cross beater mill best meets the requirement of a small $x_S/x_{S,i}$ ratio at low mass-related energy consumptions E_M for the investigated material quartz sand. Experiments in the ball mill lead to similar comminution progresses and $x_S/x_{S,i}$, ratios, but the mass-related comminution energies are clearly higher than in the cross beater mill. This is in accordance with expectations as more energy is dissipated in the ball mill. In comparison to the two other mills investigated, the single shot experiments in the Pulsar result in less comminution illustrated by higher $x_S/x_{S,i}$ ratios in Fig. 4. As the number of stress events in the Pulsar single shot experiments are much lower than in the investigations performed in the cross beater and the ball mill, the three grinding apparatus do not cover a common range of $x_S/x_{S,i}$ ratios. For that reason another criterion has to be applied in order to compare the grinding apparatus in terms of grinding energy consumption.

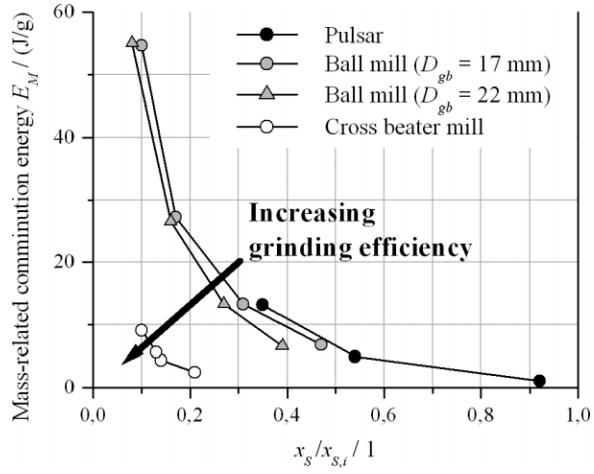

Figure 4. Comparison of mass-related comminution energy E_M.

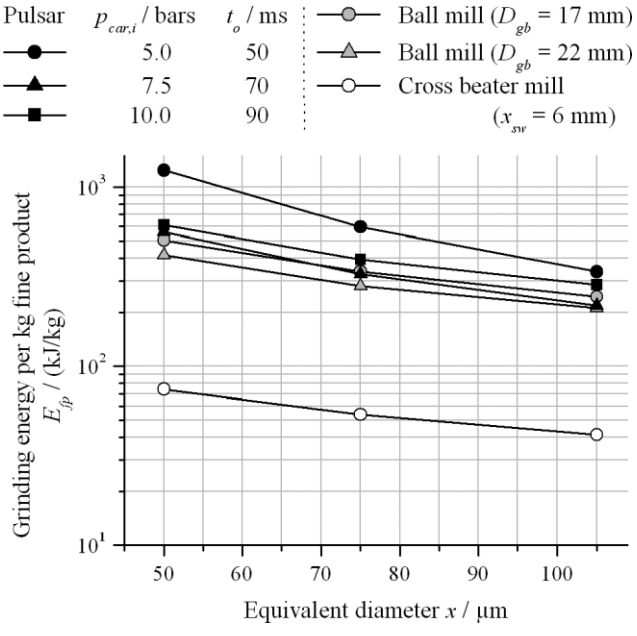

Figure 5. Comparison of grinding energy per kg of fine product E_{fp}.

In Fig. 5 the grinding energy required for the production of one kilogram of fine product below certain particle sizes (e.g., equivalent diameter by laser light scattering spectroscopy $x < 50$ µm) is displayed as a function of particle size or equivalent diameter.

Fig. 5 shows that grinding of quartz sand in the cross beater mill is far more efficient than in the Pulsar and the ball mill, resulting in lower grinding energy consumptions for the formation of fine product of the chosen particle sizes. Except for the highest mass-related energy input E_M in the Pulsar ($p_{car,i}$ = 10.0 bars, t_o = 90 ms) the relation between the grinding energies E_{fp} of the different mills is almost constant for the illustrated range of particle size (50 µm < x < 105 µm).

For the medium pressure of compressed air $p_{car,i}$ = 7.5 bars and the medium magnetic valve opening time t_o = 70 ms the grinding energy per kg of fine product E_{fp} is in the same order of magnitude as for the ball mill. Extremely low compressed air pressures $p_{car,i}$ and magnetic valve opening times t_o result in an ineffective comminution process as the required medium mass-related energy E_M for the comminution of quartz sand is hardly reached. The grinding efficiency in the Pulsar decreases with extremely increasing the compressed air pressure $p_{car,i}$ and the magnetic valve opening time t_o. This can be explained by the ineffective expansion of a large volume of compressed air which does not contribute to the comminution progress.

4 Conclusions

The present work allows for the classification of the grinding apparatus Pulsar in the field of mills in terms of energy consumption. For the grinding of quartz sand, the grinding energy per kg of fine product E_{fp} below a certain particle size (x < 105 µm) of the Pulsar and a Bond ball mill is approx. one order of magnitude higher than that of a cross beater mill, indicating much higher energy dissipations. For a compressed air pressure $p_{car,i}$ = 7.5 bars and a magnetic valve opening time t_o = 70 ms the grinding of quartz sand in the Pulsar is as efficient as in the Bond ball mill. Extremely increasing or decreasing the compressed air pressure $p_{car,i}$ and the magnetic valve opening time t_o results in less effi-

cient comminution and increased grinding energy consumptions. Therefore, the Pulsar should be operated at medium compressed air pressures $p_{car,i}$ and magnetic valve opening times t_o for the grinding of materials with properties similar to quartz sand.

Acknowledgements

The authors wish to thank the AiF for financial support of this work. They further thank Pulsar GmbH Micronizing Systems for sponsoring the Pulsar grinding apparatus.

Received: October 25, 2005

Symbols used

D_{gb}	[m]	grinding ball diameter (ball mill)
E_{fp}	[J/kg]	grinding energy per kg of fine product with particle size lower than a certain equivalent diameter
E_M	[J/kg]	mass-related energy
g	[m/s^2]	acceleration of gravity
j	[–]	interval of particle size distribution
l	[m]	length of lever arm (ball mill)
m_l	[kg]	mass on force measuring device (ball mill)
M	[kg]	mass of material
n	[–]	number of rotations (ball mill)
$p_{car,i}$	[Pa]	pressure in compressed air reservoir before shot (Pulsar)
$p_{car,f}$	[Pa]	pressure in compressed air reservoir after shot (Pulsar)
P	[W]	real power consumption (cross beater mill)
P_0	[W]	real power consumption without grinding material (cross beater mill)
Q_3	[–]	cumulative mass distribution
t	[s]	grinding time
t_o	[s]	magnetic valve opening time (Pulsar)
V_{car}	[m^3]	volume of compressed air reservoir (Pulsar)
ΔV_N	[m^3_N]	compressed air consumption per shot (Pulsar)
x	[m]	equivalent diameter, particle size
x_{sw}	[m]	sieve insert mesh width (cross beater mill)
$x_{m,j}$	[m]	mean value of interval j
x_S	[m]	Sauter mean diameter
$x_{S,i}$	[m]	Sauter mean diameter of initial material
δ_0	[–]	solids fraction of bulk
κ	[–]	adiabatic exponent
ρ	[kg/m^3]	density

References

[1] H. Rumpf, *Chem. Ing. Tech.* **1965**, *37 (3)*, 187. DOI: 10.1002/cite.330370303
[2] R. M. Schüßler, G. Hefle, *Proc. of the 10th Eur. Symp. on Comminution*, Heidelberg, Sep. **2002**.
[3] K. Schönert, *personal notice*, May **2003**.
[4] A. Weber, H. Nirschl, *Chem. Ing. Tech.* **2004**, *76 (12)*, 1806. DOI: 10.1002/cite.200407034
[5] F. C. Bond, *Brit. Chem. Eng.* **1961**, *6*, 378.
[6] F. C. Bond, *Brit. Chem. Eng.* **1961**, *6*, 543.
[7] R. Rosen, *Diploma*, Georg-Simon-Ohm Fachhochschule, Nürnberg **1988**.

